4-15-2005

Assessment of Invasive Activities of Ovarian Cancer Cells In Vitro

Hetal Shah
University of South Florida

Assessment of Invasive Activities of Ovarian Cancer Cells In Vitro

by

Hetal Shah

A thesis submitted in partial fulfillment
of the requirements for the degree of
Master of Science
Department of Physics
College of Arts and Sciences
University of South Florida

Major Professor: Chun-Min Lo, Ph.D.
Garrett Matthews, Ph.D.
Martin Muschol, Ph.D

Date of Approval:
April 15, 2005

Keywords: Invasion, ECIS, HUVECs, Metastasis, Electrode-array

DEDICATION

To my parents and my husband

ACKNOWLEDGEMENTS

On the auspicious occasion of achieving my goal of present work, I bow before God and express my deep obligations for his divine grace I offer my deep sense of gratitude to my research guide Dr. Chun-Min Lo; he has been more than a precious advisor and a great teacher to me. His leadership and guidance have given me a great sense of insight. I am highly indebted to members serving on my committee, Dr. Garrett Matthews and Dr. Martin Muschol .I express my sincere thanks to Dr. Mukherji, the chair of Physics department for his generosity and help. I also would like to express my gratitude to Dr. Yip to help us store the cells to $-80^{o}C$ and to provide HOSE cells. A special thanks goes to Sue Wolfe and Evelyne Keeton-Williams for their assistance from the moment I first attended the University of South Florida. I am also thankful to all faculty and staff of the Physics department for their support. I pay my warm and sincere thanks to my respectable parents and the whole family for encouraging and supporting me throughout my carrier. Last and not the least I thank my wonderful husband Raj, without whose help this degree was just impossible for me.

TABLE OF CONTENTS

List of Tables

LIST OF FIGURES

ASSESSMENT OF INVASIVE ACTIVITIES OF OVARIAN CANCER CELLS IN VITRO

Hetal Shah

ABSTRACT

The interactions between neighboring cells and between cells and their attached substrate have long been studied in tissue culture. These in vitro studies may provide information regarding cell behavior in vivo including cell movement, cell proliferation, tissue development and wound healing. Transcellular resistance (or impedance) measurements, using various dc or ac techniques have been used to study the barrier function of epithelial and endothelial cell layers. With an appropriate equivalent circuit used for data analysis, junctional resistance between cells and other cellular properties, including cell membrane capacitance, can be determined. However, these techniques have seldom been applied to fibroblastic cell layers because the transcellular resistance is so small that it is difficult to measure it accurately.

This research is based on detecting the invasive activities of metastatic cells in vitro using electric cell-impedance sensing (ECIS). The metastatic cells where added over the established endothelial cells and

were observed to attach and invade the cell layer. Human umbilical vein endothelial cells (HUVECs) were first grown and then loaded on eight well gold electrodes. The impedance of these electrodes was followed after the suspension of different sublines of cancer cells (SKOV3, OVCA429). For highly metastatic sublines, within an hour after being challenged, the impedance of confluent HUVECs layer was substantially reduced. In addition the conditioned cancer media and heat-killed cancer cells was also suspended which had no substantial effect on the impedance. This result suggests that ECIS based assay might be used with primary human cultures to establish the metastatic abilities of cells.

CHAPTER 1

Introduction and Background

One problem of central importance in United States is cancer, especially ovarian cancer. According to the National Cancer Institute each year more than 22,000 women in the United States develop ovarian cancer. What Is Cancer? Cancer is a group of more than 100 different diseases. They all affect the body's basic unit, the cell. Cancer occurs when cells become abnormal and keep dividing and forming more cells without control or order.

Like all other organs of the body, the ovaries are made up of many types of cells. Normally, cells divide to produce more cells only when the body needs them. This orderly process helps keep us healthy. If cells keep dividing when new cells are not needed, a mass of tissue forms. This mass of extra tissue, called a growth, or tumor, can be benign or malignant. Benign tumors are not cancer. They can usually be removed and, in most cases, they do not come back. Most important, cells from benign tumors do not invade nearby tissues and do not spread to other parts of the body. Benign tumors are rarely life threatening. Malignant tumors are cancer. Cancer cells can invade and

damage tissues and organs near the tumor. Also, cancer cells can break away from a malignant tumor in the ovary and spread to other organs in the abdomen and form new tumors. Ovarian cancer spreads most often to the colon, the stomach, and the diaphragm. The cancer cells also can enter the lymphatic system or the bloodstream and spread to other parts of the body. The spread of cancer is called metastasis.

When cancer spreads, the new tumor has the same kind of abnormal cells and the same name as the original (primary) tumor. For example, ovarian cancer that spreads to the colon is metastases ovarian cancer. It is not colon cancer, even though the new tumor is in the colon. The growth of large tumor is dependent on abnormal cells that exhibit uncontrolled growth and development of endothelial cells to undergo angiogenesis. This allows the mass to grow beyond the constraints imposed by diffusion (1). The problem to consider is the interaction between neighboring cells and matrix (substrate) to which they attach. One aspect of this concerns cell locomotion, as many types of mammalian cells have the ability to move about the surfaces. The exact mechanism accounting for this motion is not fully understood, but it has been demonstrated to involve muscle-like filaments that transverse the interior of the animal cell. Both cell-surface interactions and cell locomotion are phenomena that are extremely important in

developmental biology, as well as in adult cellular activities such as wound healing. In addition, these activities undoubtedly play a major role in the metastases behavior of cells in malignant tumors. Several studies have reported a link between the metastatic behavior of cancer cells and their motility in culture (12-14). Such correlations will be of eloquence both in studying the metastatic process and in devising clinical measurements for treatment of cancer. These problems have long been studied in tissue culture, where microscopic visual observations of cell morphology and determination of cell number are employed. Cell motility has traditionally been followed using cinematographic time-lapse methods.

Several years ago Kramer and Nicolson presented scanning electron micrographs demonstrating, in cell culture, the metastatic-like behavior of cancer cells. In this work they first established a confluent layer of bovine aortic endothelial cells (BAE) in culture. This cell layer was then challenged with highly metastatic cells like B16 melanoma cells. Electron micrographs taken at different time intervals showed the melanoma cell attaching to the endothelial cell layer, with subsequent retraction of the endothelial cells, and finally penetration of the melanoma to the tissue culture substratum. This activity in vitro refers to the similar activity in vivo that takes place during the metastatic process. This technique provides information about the

behavior of metastatic cells but lack to provide information in real time regarding dynamics of the process.

Over the last 20 years, several reports have described the use of this technology for monitoring cellular events, including macrophage adherence and spreading upon activation, endothelial cell shape changes for assessment of its barrier function, cell micromotion, cell morphology changes due to various factors such as cytoskeletal rearrangement, cell spreading on different surfaces, cell migration and cell responses to cyto-toxic compounds (5). Previously, related work on the electrical characteristics of continuous sheets of epithelial cells growing on permeable supports has been reported (6,7). In other studies involving an elegant array of small electrodes, Thomas et al (8) have monitored the bioelectrical activity of cultured embryonic chicken heart cells. However, these studies did not report the use of externally applied electric fields to detect the cell spreading and its motion.

An electrical method useful to easily detect this alteration in the endothelial cell layer, referred as Electric cell-substrate impedance sensing (ECIS) first described by Giaever and Keese (Applied Biophysics, Troy, NY) has been developed to look for correlations of impedance changes with the metastatic potential of cells for real time

measurement of the changing impedance properties of attached and spreading cells that act as insulating particles on gold electrodes.

While such a small ac current exhibits no adverse effect on the activity, survival and response of cells to diverse stimuli, cells in contact with the small gold detecting electrode act as insulating particles [1–4]. To date, ECIS has been proven as a versatile and noninvasive tool for real time measurement of changes in the impedance associated with cell behavior [1–4]. We have applied the present ECIS method to study the invasive activity of ovarian cancer cells with great sensitivity. According to the previous results we know that the cells attach essentially in the same way as they do in the normal culture dishes made from treated polystyrene so the results obtained from the ECIS measurements are both consistent and clear. Using ECIS, we studied the attachment and spreading of HUVECs, the change in electrical impedance when HUVEC cells were challenged with ovarian cancer cells, conditioned medium, and heat-killed ovarian cancer cells. In distinction to other methods used for cell attachment studies, ECIS can follow the cell behavior continuously and noninvasive for hours, so that certain long term characteristics of cell attachment and spreading are noticed that has not been considered in traditional assays (9). Giaever and Keese in 1984, designed a new electrical method to monitor fibroblastic behavior in vitro. Mammalian fibroblasts

were cultured on evaporated gold electrodes driven with an alternating electric field at 4000 Hz (7). The dish used consisted of one large (~ 2 cm^2) and four small (~ 3×10^{-4} cm^2) electrodes bathed in tissue culture medium. The applied electric field produced a voltage drop of a few mA/cm^2 at the boundary between the solution and the small electrode. The authors suggested that the small population of cells that had attached and spread on the small electrodes had a marked effect on the measured impedance and caused it to fluctuate with time. The amplitude of these fluctuations was greatly reduced by cytochalasin B (10 μM), suggesting they were a consequence of cell movement. Later in 1986 the same studied the attachment and spreading of two cell types, one normal cell, WI-38, and one transformed cell, WI-38 VA13 (24). They studied the cells response to various protein-covered electrodes in which they found that fibronectin and gelatin proved to be good substrates for most cell types. By studying the fluctuations of the in-phase voltage they detected the motion of the cells. The transformed cells shifted their anchoring of the surface more often than the normal cells. In 1991, Giaever and Keese studied micromotion of mammalian cells (11), where they showed that average motion of the cell layer of 1 nm could be inferred from the ECIS measurements. In 1997 Lo and Ferrier studied the impedance analysis of fibroblastic cell layers (22). Here they proposed an

extended model of impedance analysis for cell layers where cells are considered rectangular. Moreover they measured average cell-substrate separation of human gingival fibroblasts at different temperatures. In 2000, Wegener et al. used ECIS as a noninvasive means to monitor the kinetics of cell spreading to artificial surface (23) in which they studied the attachment and spreading of epithelial MDCK cells (strain II) on different protein coatings, and investigated the influence of divalent cations on spreading kinetics. They quantified the inhibitory effect of soluble peptides that mimic the recognition sequence of fibronectin and other extracellular matrix proteins (RGDS). They also applied the ECIS technique to monitor the detachment of confluent fibroblastic cell layers (WI38/VA-13) by means of these peptides. In 2002 Keese et al. used the real-time impedance assay to follow the invasive activities of metastatic cells in culture (4). In their work, the Human Umbilical Vein Endothelial cells (HUVECs) were first grown to confluence on small gold electrodes. The impedance of these electrodes was taken after the suspensions of different sublines of dunning murine prostatic adenocarcinoma series (G, AT1, AT2, AT3, ML, and MLL). They found that for highly metastatic sublines, within an hour after being challenged, the impedance of confluent HUVEC layer was substantially reduced. The effect of the weakly metastatic sublines was less pronounced, and the

extent and the rate of this drop in impedance could be correlated with the metastatic potential of each of the six sublines tested.

Starting from 1991 till now, many applications of ECIS and their experimental results have been shown. The entire work stated above suggests that ECIS is powerful electric technique to study the cell behavior in tissue culture.

CHAPTER2

Materials and Methods

2.1 Instrumentation

The ECIS core technology is based on a technique of measuring the change in impedance of a small electrode to AC current flow. The heart of the measurement is a specialized slide that has 8 individual wells for cell culturing. The base of the device has an array of gold film electrodes that connects the ECIS electronics to each of the 8 wells. The current flows between a 250 μm diameter electrode and a larger counter electrode using normal culture medium as the electrolyte. The leads from one of the small electrodes and large electrodes were connected to a SR830 lock-in amplifier from Stanford Research Systems. To study cell morphological changes, usually a 1V 4000 Hz AC signal through a 1 MΩ resistors was used to provide an approximately constant current of 1 μA through the system. All connections were done by coaxial cable to minimize any background noise. The setup is shown in Fig.2.1. As the cells attach and spread on the electrode, it changes the impedance in such a way that morphological information about the attached cells can be inferred.

2.2 Experimental Setup

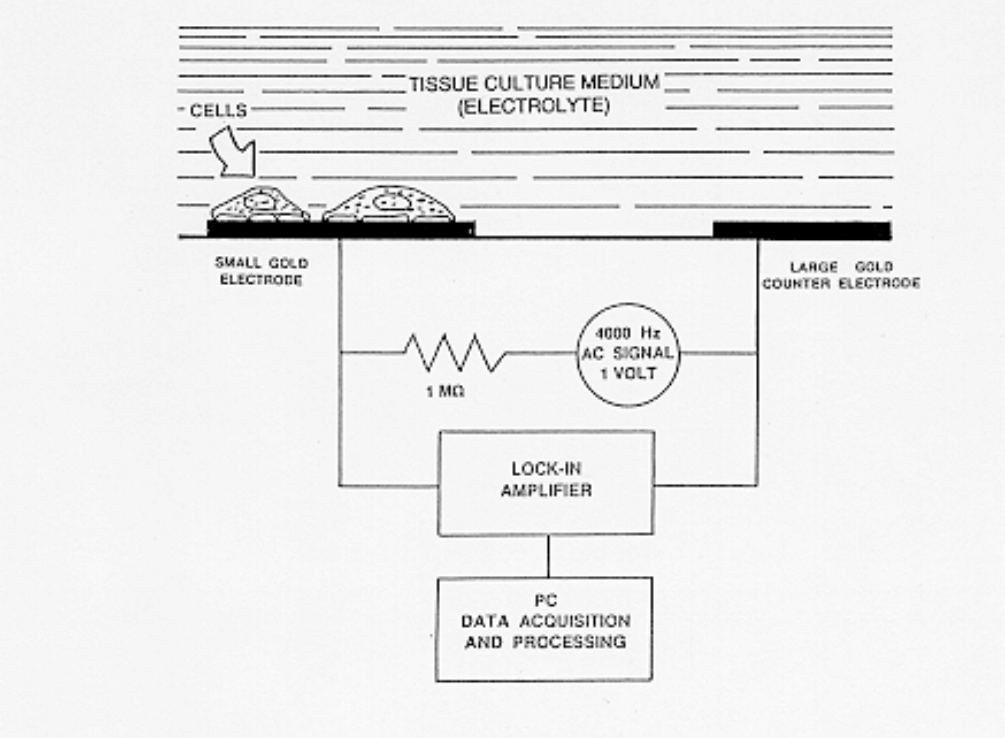

Fig.2.1 Impedance of small electrode is measured with a lock-in amplifier in series with 1 MΩ resistor to obtain approximate constant current.

In addition to the impedance measurements the data were also converted to resistance and capacitance, considering the cell electrode system as a simple resistor and capacitor in series. When the cells attach and spread upon the electrode, they block the current. This compels the current to flow beneath and between the cells and result in large increase in impedance. Since the microampere currents and the resulting voltage drop of a few millivolts have no measurable effect on the cells, the monitoring of the cell behavior is noninvasive (10).

2.3 Electrode Array

Each electrode well used for the ECIS measurements is well explained by Keese et.al. (10). All eight electrode contains small working electrode (area= 5×10^{-4} cm^2) and a large counter electrode (area=0.15 cm^2). Because of the difference in surface area, the impedance of the small electrode determines the total impedance of the system. The active electrode is delineated by circular openings (diameter = 250 μm) in a photoresist overlayer that insulates the rest of the deposited gold film from bulk electrolyte. As cells in the culture attach to the electrode, we can relate the cell behavior by the impedance measured by this device. We selected the size of the electrode to be this small as cell related signals are difficult to measure

with large electrodes. This is because solution resistance in the culture dish is much larger than the electrodes impedance. The impedance of the electrode electrolyte interface (Faradaic impedance) is proportional to the inverse of the electrode area, but constriction resistance (spreading resistance) for the circular disk electrode in a conducting medium of infinite extent varies as $\rho/2d$, where ρ is the resistivity of the medium and d is the diameter of the electrode. So the electrode impedance can always be made to dominate the constriction resistance by using sufficiently small electrodes. When the electrode area is reduced to 10^{-4} cm^2, the Faradaic resistance of the electrode-electrolyte interface at 4000 Hz is many times larger than the constriction resistance so the motility of the cells can be easily studied. The image of the electrode we used in our lab is given in Fig.2.2 A.

(A)

Fig.2.2.A. Eight well electrode

(B)

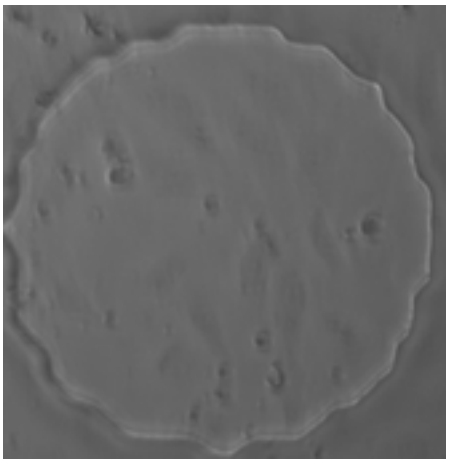

Fig.2.2 B. Microscopic view of HUVECs in the electrode

2.4 Cell Culture Procedures

Samuel MOK at Harvard Medical School supplied us HOSE15 (a primary culture of normal human ovarian surface epithelial cells), OVCA429 (a primary culture of ovarian carcinoma cells), and SKOV3 (an ovarian cancer cell line) cells in frozen ampoules. These were thawed and grown in medium 199 and MCDB 105 (1:1) (Sigma) supplemented with 10% fetal calf serum (Sigma), 100 units/ml penicillin, and 100 μg/ml streptomycin under 5% CO_2, and 37^0C, high-humidity atmosphere. The Human Umbilical Vein Endothelial Cells (HUVECs) were obtained from Clonetics Corp. and were grown in endothelial cell growth which is added with following: 10 ng/ml human recombinant Epidermal Growth Factor, 1 μg/ml hydrocortisone, 50 μg/ml getamicin, 50 ng/ml amphotericinB, 12 μg/ml bovine brain extract and 2% fetal bovine serum (amounts indicate final concentration). For the ECIS studies the cells were taken from slightly subconfluent culture usually 48 hrs after passage. The culture medium was changed twice a week. Cell suspension was prepared using standard tissue culture technique with 0.05% or 0.25% of trypsin/EDTA. The cells were then kept in the incubator to equilibrate before adding to each wells of the electrode.

2.5 Cell Attachments And Spreading

The suspension of HUVECs in the wells was prepared from the confluent cell layers. The cells were first washed with Hanks' Balanced Salt solution of nearly 5 ml. The cells were then kept in the incubator with 0.05% of trypsin (2.5 ml) in it. Adding nearly 4 ml of the complete culture medium terminated the trypsinization. The cells were then spun down at 1500 rpm for 5 min. These made the cells to settle down. The media with trypsin in the cell was separated. Fresh culture media was then added and density of the cells was known by using standard hemacytometer. The impregnate was adjusted to give a final cell number of 9×10^4 cells and final cell density in each well of 10^5 cell/cm^2. Before suspending the cells the electrode was coated with gelatin and kept in the incubator for 15 min. A solution of 200 μg/ml gelatin in 0.15 M NaCl was used. Gelatin settled down and protein solution was then aspirated. The electrode-containing wells were rinsed twice with the culture medium. Prior to inoculation, ECIS electrodes were rinsed with small amount of serum free culture medium. The Fig.2.2.B. shows the attachment of the HUVEC cells to the electrode. The image was taken 24 after inoculation of 10^5 cells/cm^2 HUVEC cells into the well

2.6 Cancer Invasion Assay

We also used ECIS to monitor the effect of OVCA429, SKOV3, and HOSE cells on cell-substrate adhesion of already attached HUVEC cell layers and to follow cell detachment from the substrate. The cell confluence was verified both microscopically and by ECIS measurements. The HUVECs were generally incubated for 1-2 days before the OVCA429 and SKOV3 cells challenge. Impedance measurements were used to test that confluence was achieved, maintained and that the cells exhibited normal levels of impedance fluctuations indicative of healthy cell layers (15). The detachment data were then run for 90 min with just the HUVEC cells to establish a baseline. Before the challenge of cancer cells, they were allowed to grow in the culture dish for 2 days to reach confluence. The cells were then trypsinized with 0.25% (2.5 ml) trypsin for OVCA429 and 0.05% (2.5 ml) trypsin for SKOV3 cells. They were then kept in the incubator for 7 mins (OVCA429) and 5 mins (SKOV3). The complete cancer medium (4 ml) was then added to neutralize the effect of trypsin. The cells were then spun at 1500 rpm for 5 mins. We saw that the cells settled down. The medium with the trypsin was then aspirated and the new cancer cell complete medium was added. We then counted the cells with hemacytometer (added more media to make the total cell density as 10^5 cells/cm^2). The Fig.2.4 shows normal HUVECs and

different cancer cells in the culture dish that were taken for the ECIS measurement. The image shown was taken with cells in culture dish 24 hrs after subculture.

(A) (B)

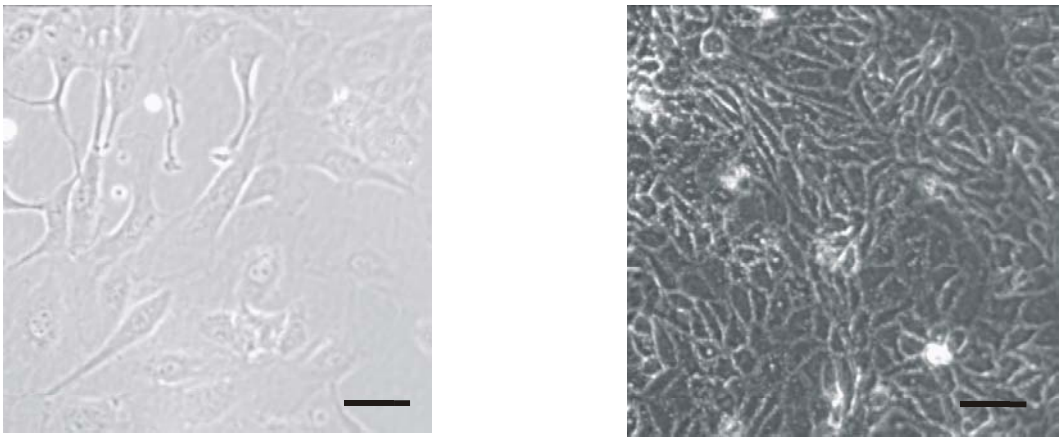

(C) (D)

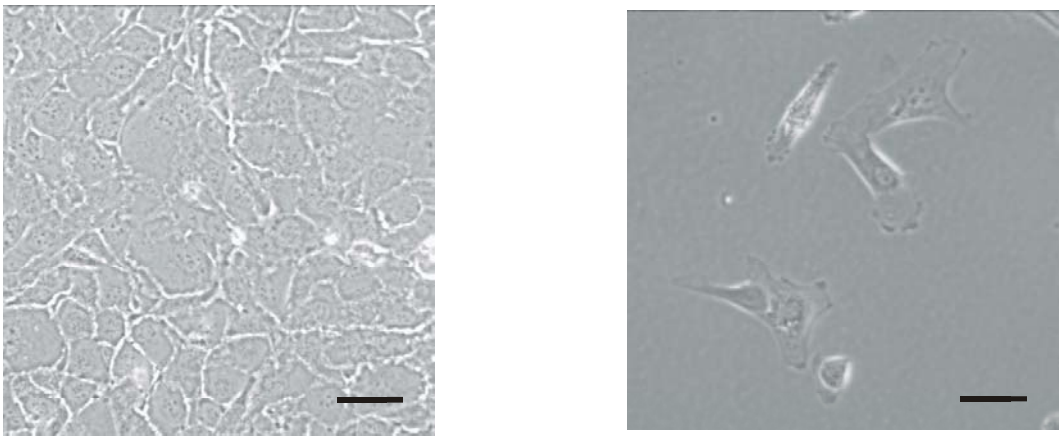

Fig. 2.3 Microscopic view of (A) HUVEC (B) OA429 (C) SKOV3 and (D) HOSE15 cells attached to the electrode. The image was taken 24 hrs after culture. The scale bar marked in the figure is 50 μm.

2.7 Conditioned Medium of SKOV3 and OVCA429

The culture medium that keeps the OVCA429 and SKOV3 cells confluent was taken from the culture dish kept in the incubator after 3 days of subculture. It was centrifuged at 1500 rpm for 5 minutes. This process made the cells (if present) settle down leaving just the medium on the top of the tube. This medium was then replaced after removing 250 μl medium from the electrode well that contains the confluent HUVEC layer.

2.8 Heat-killed SKOV3 cells and OVCA429

To study the cause of the HUVEC cell layer that altered the resistance value, the OVCA429 and SKOV3 cells were first taken from the culture dish and passed to trypsin (0.25% (2.5 ml) for OVCA429 cells and 0.05% (2.5 ml) for SKOV3 cells). They were then kept in the incubator at 37^0C for 5 (SKOV3) and 7 (OVCA429) minutes. We then added 4 ml complete medium for cancer cells to neutralize the effect of trypsin. The medium with trypsin was then aspirated and the new HUVEC complete medium was added. We then counted the cells with the hemacytometer and added more media to make the total cell density of 10^5 cells/cm^2 to keep the ratio of HUVEC to cancer cells as 1:1. The cells were then heat killed at 55^0C for 15 min. They were then allowed to cool to room temperature and 0.2 ml of this suspension was added

to the already established HUVEC culture. To compare the data we used one electrode as control with the same amount of HUVEC complete medium to make the total volume equal in all wells.

Chapter 3

Model Derivation and its Parameter

3.1 ECIS Theoretical Model

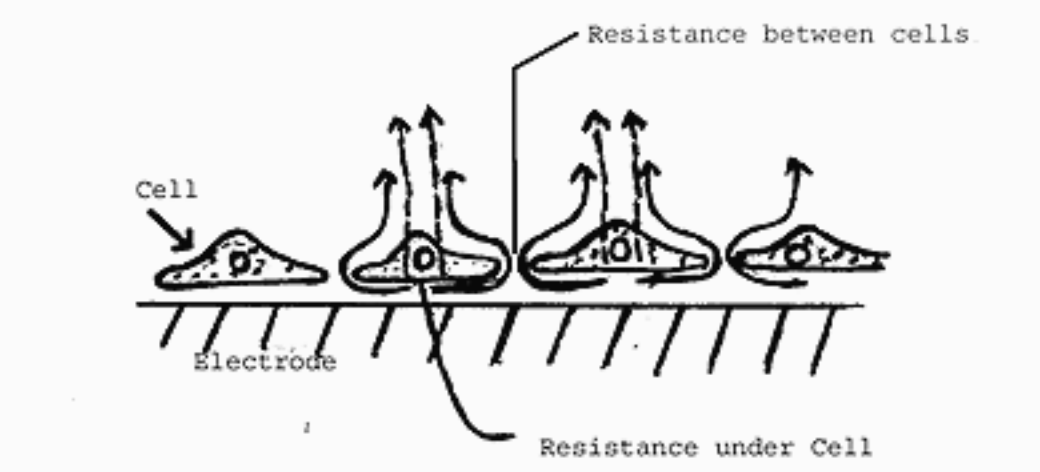

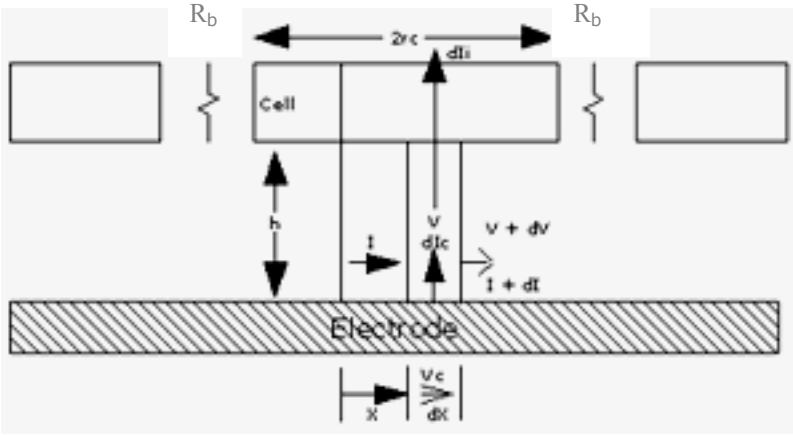

Fig.3.1 Model of the cells in tissue culture emphasizing space between the cell and substratum. Calculated resistance is due to the current flow under the cells and an additional resistance because the current must flow out between the cells. Broken line represents the capacitive current flow through the membranes. The cells are regarded disk shaped and viewed from top. ρ is the resistivity of solution.

Fig.3.1 shows a schematic of the electrodes and the basic electrical setup used in these measurements. The model derivation for the ECIS has been well explained by Giaever and Keese in 1991 (16). In this two-probe electronic instrument, the resistance of the bulk tissue culture medium is in series with the impedance of the electrodes and will govern the measurement except when an electrode is small. The solution resistance will then be shown itself as a spreading or constriction resistance that depends on the size of the electrode. Take an example, for a circular disk electrode in a conducting medium of large radius, the constriction resistance varies as $\rho/2d$, where ρ is the resistivity of the medium and d is the diameter of the electrode (17). As the impedance measured with the electrode-electrolyte interface should be inversely proportional to the area of the electrode, $4/\pi d^2$, it can always govern the constriction resistance by making the diameter sufficiently small. For an electrode of 10^{-3} cm^2, the real part of the impedance of the electrode (the faradaic resistance) is several times larger than the constriction resistance at 4 kHz. Under these conditions, the activities of attached cells are clearly studied. If two large electrodes had been used, the solution resistance would have concealed the measurement and the presence of cells would be barely noticed. The model used to calculate the specific impedance for a unit area of a cell-covered electrode as a function of the frequency ν, is

shown in Fig. 3.1. It depends on the measured specific impedance $Z_n(\nu)$, of a cell-free electrode, the specific impedance $Z_m(\nu)$, through the cell layer which is mainly the capacitance of the upper and lower cell membranes in series and the resistivity p, of the tissue culture medium. The cells have been considered as circular disks of radius r_c. We considered that the current flows radially in the space formed between the ventral surface of the cell and the substratum and that the current density under the cells does not change in the z direction. The equations can be stated as

$$-\frac{dV}{dr} = \frac{\rho}{h2\pi r} I$$

$$V_c - V = \frac{Z_n}{2\pi r dr} dI_c$$

$$V = \frac{Z_m}{2\pi r dr} dI_i$$

$$dI = dI_c - dI_i$$

This equation can be combined to yield

$$\frac{d^2V}{dr^2} + \frac{1}{r}\frac{dV}{dr} - \gamma^2 V + \beta = 0$$

here

$$\gamma^2 = \frac{\rho}{h}(\frac{1}{Z_n} + \frac{1}{Z_m})$$

and

$$\beta = \frac{\rho V_c}{hZ_n}$$

Where V_c is the potential of the electrode, and h is the height of the space between the ventral surface of the cell and the substratum. The solution of above equation is a sum of modified Bessel functions of first and second kind (18). Using proper boundary conditions, the specific impedance for a cell-covered electrode is obtained as follows:

$$\frac{1}{Z_c} = \frac{1}{Z_n}[\frac{Z_n}{Z_n + Z_m} + \frac{\frac{Z_m}{Z_n + Z_m}}{\frac{\gamma I_c}{2}\frac{I_0(\gamma r_c)}{I_1(\gamma r_c)} + R_b(\frac{1}{Z_n} + \frac{1}{Z_m})}]$$

Where I_O and I_1 are modified Bessel functions of the first kind with order 0 and 1. Here the solution depends on two parameters i.e. R_b, the resistance between the cells for a unit area, and α which can be given as:

$$\gamma r_c = r_c \sqrt{\frac{\rho}{h}\left(\frac{1}{Z_n} + \frac{1}{Z_m}\right)} = \alpha \sqrt{\frac{1}{Z_n} + \frac{1}{Z_m}}$$

Since $Z_n(\nu)$ is measured and $Z_m(\nu)$ is the impedance of two cell membranes in series (see Fig.3.1). Now, α and R_b are the only adjustable parameters in the equation stated above. The expression does not depend on frequency directly but is contained in the impedances $Z_n(\nu)$ and $Z_m(\nu)$.

3.2 Frequency Scan

Frequency Scan is one of the distinct methods of ECIS that measures the impedance of the cell-electrode system as a function of frequency. To get the impedances as a function of frequency for both cell-free electrode and the same electrode with confluent cells, we ran frequency scan before and after cells attach on the electrode. The data is shown in Fig. 3.1.A. shows the resistance of cell free electrode and same electrode confluent with HUVEC cells and Fig. 3.1.B shows the capacitance of the cell free electrode and same electrode confluent with HUVEC cells. Using this model to calculate the impedance of an electrode supporting a confluent layer of cells, Z_c, we first measure the impedance of a cell-free electrode at different frequencies. It is easy to describe the measured sample impedance as equivalent to that of a capacitor and a resistor in series that was first done by Warburg (19, 20) for electrolytic interfaces. This can be shown in Fig. 3.2, which displays the measured resistance and capacitance as a function of frequency for confluent layer of HUVECs. To get the data, the electrode array was first placed in the incubator, and the medium (0.5 ml) was added to each well. The large electrode and one of the small electrodes were connected to the lock-in amplifier, and an AC signal was passed through 1 MΩ resistor Fig.2.1. As we know that the constriction resistance is in series with this impedance, we can

subtract it from the total resistance to obtain the real resistive value of Z_n. After calculating Z_c, the constriction resistance is added back for comparison with the experimental results. For analyzing difference in the impedance curve, we used the normalized values where we divide the impedance values of the cell-covered electrodes by the cell-free electrodes. The line in fig. 3.3.A and 3.3.B are the normalized resistance and capacitance curve for HUVECs. The points on the same figure are the calculated valued which depends on the model. The best fit of the graph was obtained with the value of α = (4.4) $\Omega^{1/2}$cm and R_b=(3.9 $\pm$ 0.1) Ωcm^2. Moreover the important thing to consider is that, the cells are neither circular nor rectangular. All the cells do not have the same shape. This model shows, however, that the change in impedance due to a confluent cell layer comes from two sources, one due to the current flow between the ventral surface of the cells and the substratum, and the other due to the resistance between cells.

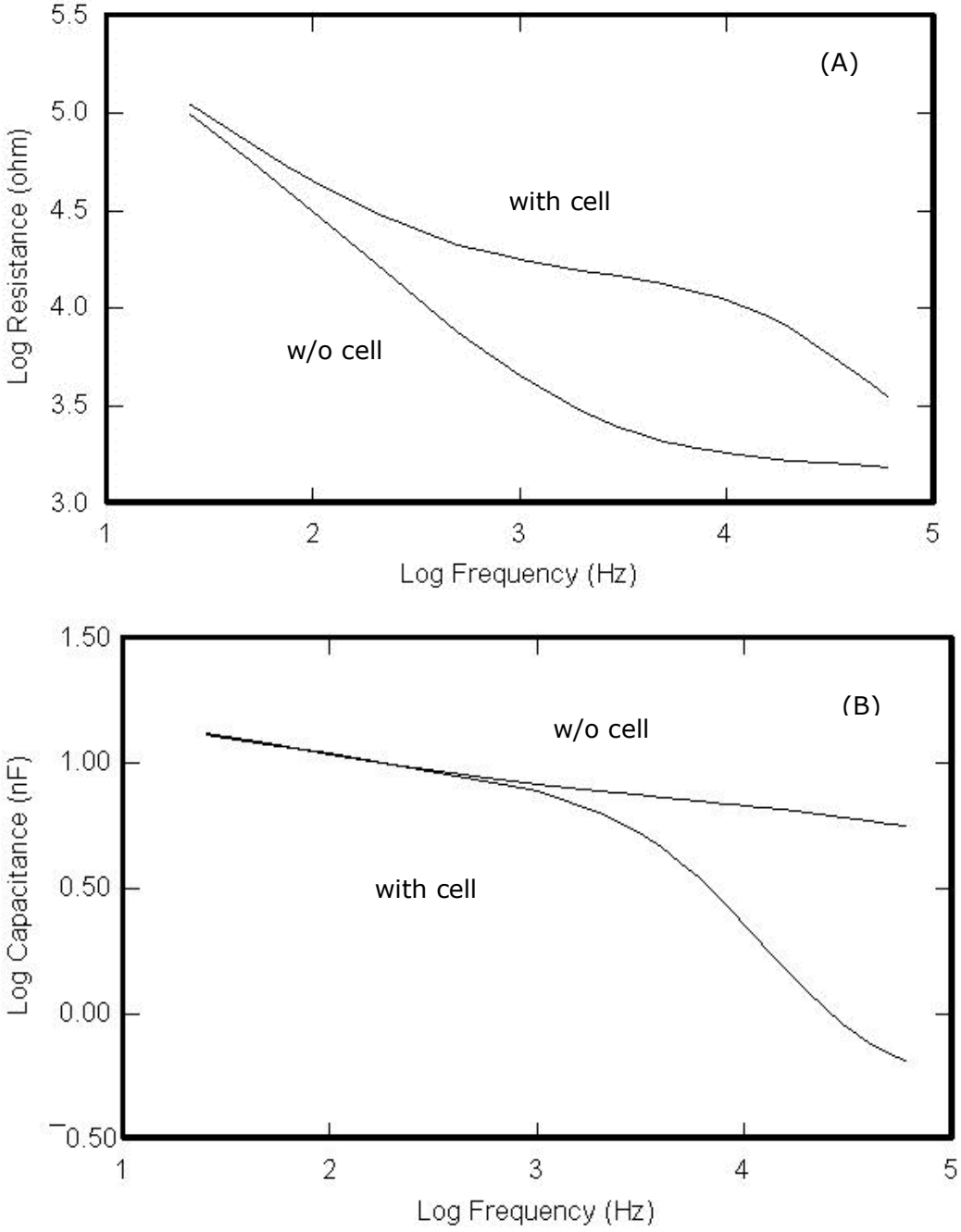

Fig.3.2 (A) Resistance and (B) Capacitance data as a function of frequency obtained from Frequency Scan measurements. The data is for with and without confluent HUVEC cells.

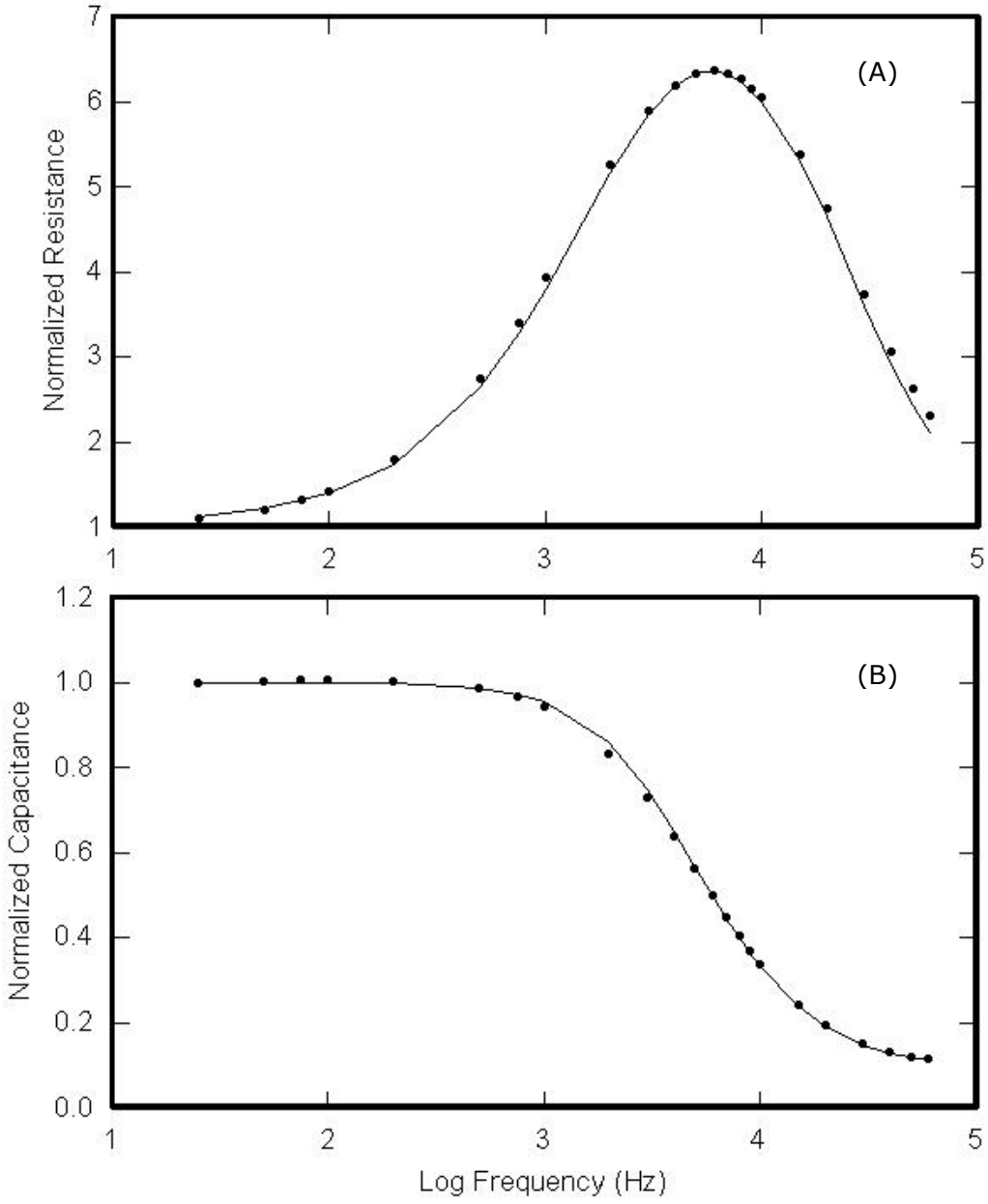

Fig. 3.3 (A) Normalized resistance and (B) normalized capacitance obtained from electrodes confluent with HUVEC cells and dividing with values for the cell-free electrodes. Black points represent calculated values.

Chapter 4

Result And Discussion

4.1 Inoculation of HUVECs

Fig.4.1. shows the initial attachment of the HUVECs. The resistance value is obtained with respect to the change in time. Seven individual electrodes were used to show the impedance measurement from the time zero when the cells were inoculated to 20 hrs period. The data were taken at frequency of 4 kHz. Initially the cells are not attached and the resistance is nearly 2000 Ω. On the inoculation of HUVECs, the cell attach to electrodes in each well. Now the insulating plasma membrane present in the cell, block the flow of the current so the current flows beneath and between the cells. This path of the current causes more change in the impedance value. This takes place at the small and the counter electrode but the impedance of the small electrode is too large compared to the larger electrode and thus can be ignored. The initial rise in the resistance is due to the cell attachment and spreading. Spreading is completed in nearly 2.5 hrs. Here from the Fig.4.1., we notice that the resistive portion of the impedance increased much higher than cell free electrode. The fluctuation

observed in the increased impedance is because the cells are alive and they change their morphology, which affect the impedance. The important thing to understand is that the ac current used for this measurement ($\cong 1$ μamp) and relative voltage drop across the cells (few millivolts) has nearly no effects so the measurements taken are noninvasive.

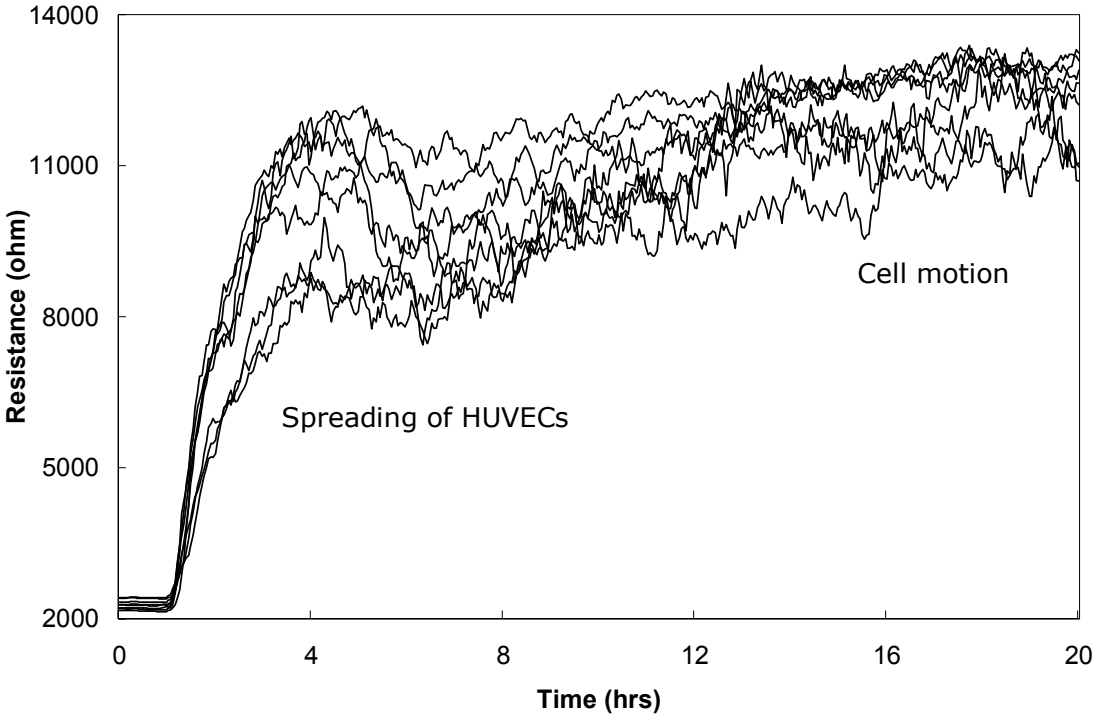

.

Fig. 4.1 Inoculation of HUVECs measured by ECIS. Measurements were made in seven independent well at 4 kHz, all the electrodes were gelatin coated.

4.2 Cell attachment and spreading of SKOV3, OVCA429 and HOSE15 cell

Fig.4.2 shows the attachment and spreading of SKOV3, OVCA429 and HOSE15 cells. The cells were added to the electrode when that electrode was not recording the data. The OVCA429 cells were highly metastatic. The data shown is the change in the resistance with respect to the time. We added nearly 10^5 cell/cm^2. We observed that the resistance of HOSE15 cells went to nearly 5000 Ω after 15 hrs of cell suspension. This acted as control and did not show any significant effect. While the resistance value of OVCA429 and SKOV3 cells reached to approximately 12000 Ω after 15 hrs of cell suspension into electrode wells. The OVCA429 cells were even tough to trypsinize. They just grow like an island with neighboring cells forming very tight junctions. This increase in resistance shows that the cancer cells attach and spread very well to the electrode. As they attach and spread to the electrode, they block the current flow and thus the current flows beneath and between the cells. As these cells forms a tight junction, the resistance value goes too high. When viewed by the microscope these cells were flattened which showed they attach and spread very well.

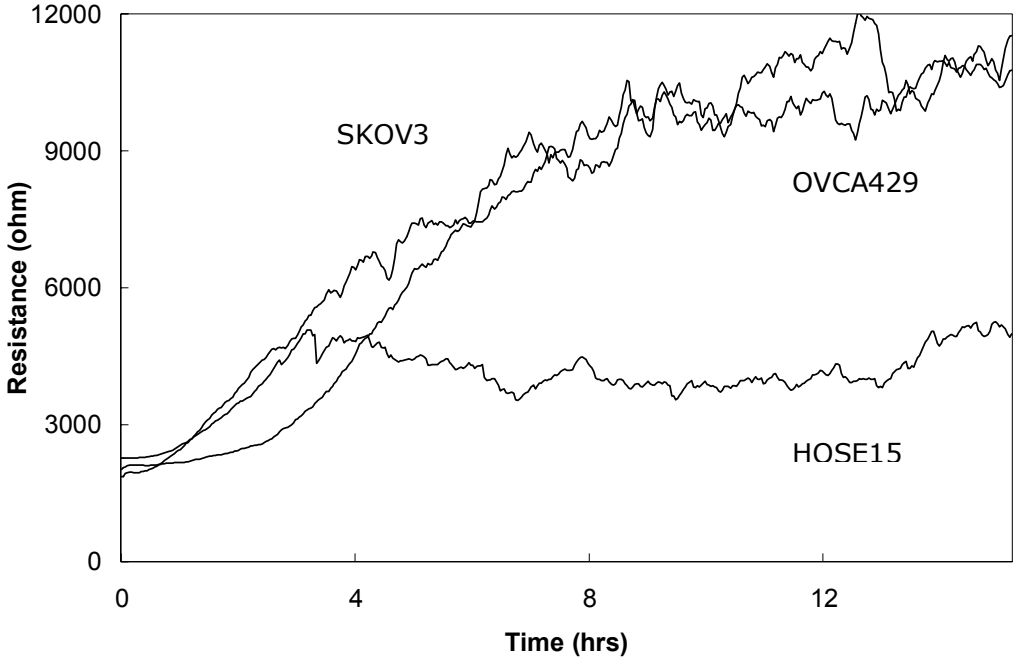

Fig.4.2. Cell attachment and spreading of SKOV3, OVCA429, and HOSE15 cells. The results shown were taken at 4 kHz.

4.3 Impedance analysis of SKOV3, OVCA429 cells

Fig.4.3 and Fig.4.5 show the real part (resistance) and imaginary part (capacitance) of the transepithelial impedance with respect to frequency. This entire figure shows the experimental data for the cells free electrode and the cells confluent with OVCA429 (Fig.4.3.) and SKOV3 (Fig.4.5) cells at 37^0C. Fig.4.4 and Fig.4.6 displays the normalized resistance and capacitance value obtained from the confluent OVCA429. Fig.4.3 and SKOV3 cells Fig.4.5 divided by the values obtained from cell free electrode. From this we calculate the impedance to cell covered electrode i.e. Z_c. As we know that the specific impedance of the cell-free electrode Z_n is function of frequency, we first measure Z_n at different frequencies. At high frequencies, a significant part of the resistive value of Z_n is the solution resistance (constriction resistance), which can be obtained by taking the asymptotic value of Z_n. Again this constriction resistance is in series with this impedance, it can be simply subtracted from the total resistance to obtain the real resistive value of Z_n. After calculating Z_c, the constriction resistance is added back for comparison with the experimental results (16). The computer software does this process and fit the data to gives the R_b and α value. The best fit for SKOV3 cells was obtained at α =6.6 $\Omega^{1/2}$cm and R_b =8.1 Ωcm^2. Since $\alpha = r_c(\rho/h)^{1/2}$, the radius of the SKOV3 cells r_c =15 μm, ρ = 60 Ωcm

(resistivity of the medium) so we calculated the height of the ventral surface of the cell and the substratum and obtained h =31 nm. The experiment was repeated many times and the average value of α, R_b and h were obtained. Similarly for the OVCA429 cells, the best fit was obtained for the α =23.3 $\Omega^{1/2}$cm and R_b =34.4 Ωcm^2. These cancer cells are smaller in size than the normal HUVECs. Here even ρ =60 Ωcm, and using an average measured radius r_c =12 μm so the channel height becomes h =1.6 nm. The channel height is dependent on the cell shape however the relative proximity of the transformed cell to the substratum compared to the normal cell is independent of the choice of the cell shape in the model (16). This very small value of h compared to the value obtained by HUVECs shows that large area of cell-substrate contact exist between caner cells and electrode. They really attach very well to the electrode and spread fast. When we add the cells to the electrode they are rounded and after nearly six hours of inoculation they start spreading and attaching to the electrode so the resistance even increase. The R_b, α ,h and C_m values of different cell types are given in Table 4.1.

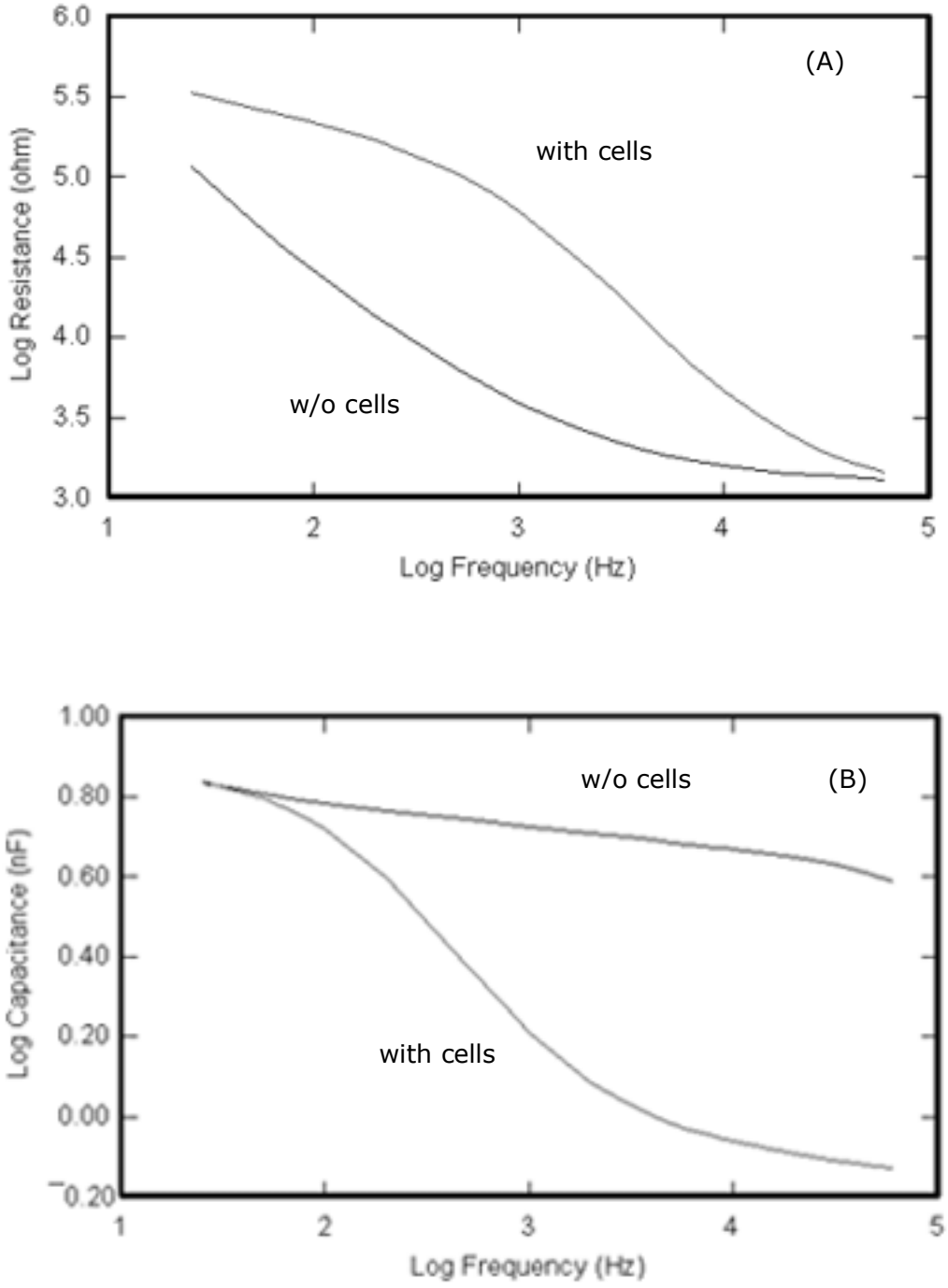

Fig.4.3.(A). Resistance and (B) capacitance data as a function of frequency obtained from Frequency Scan measurement. The data shown is with and without OVCA429 cells in the electrode.

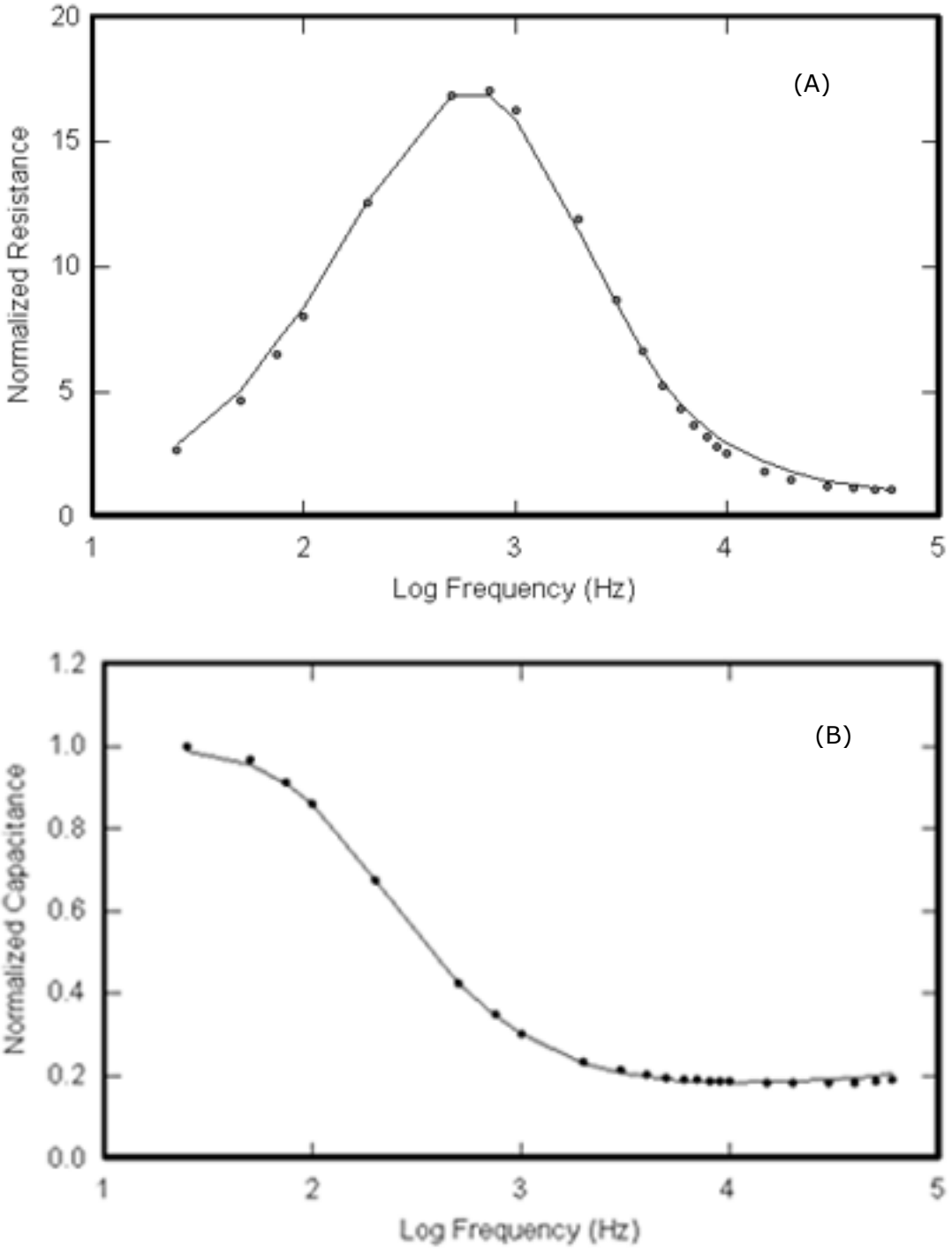

Fig. 4.4 (A) Normalized resistance and (B) Normalized capacitance from model calculation for OVCA429 cells.

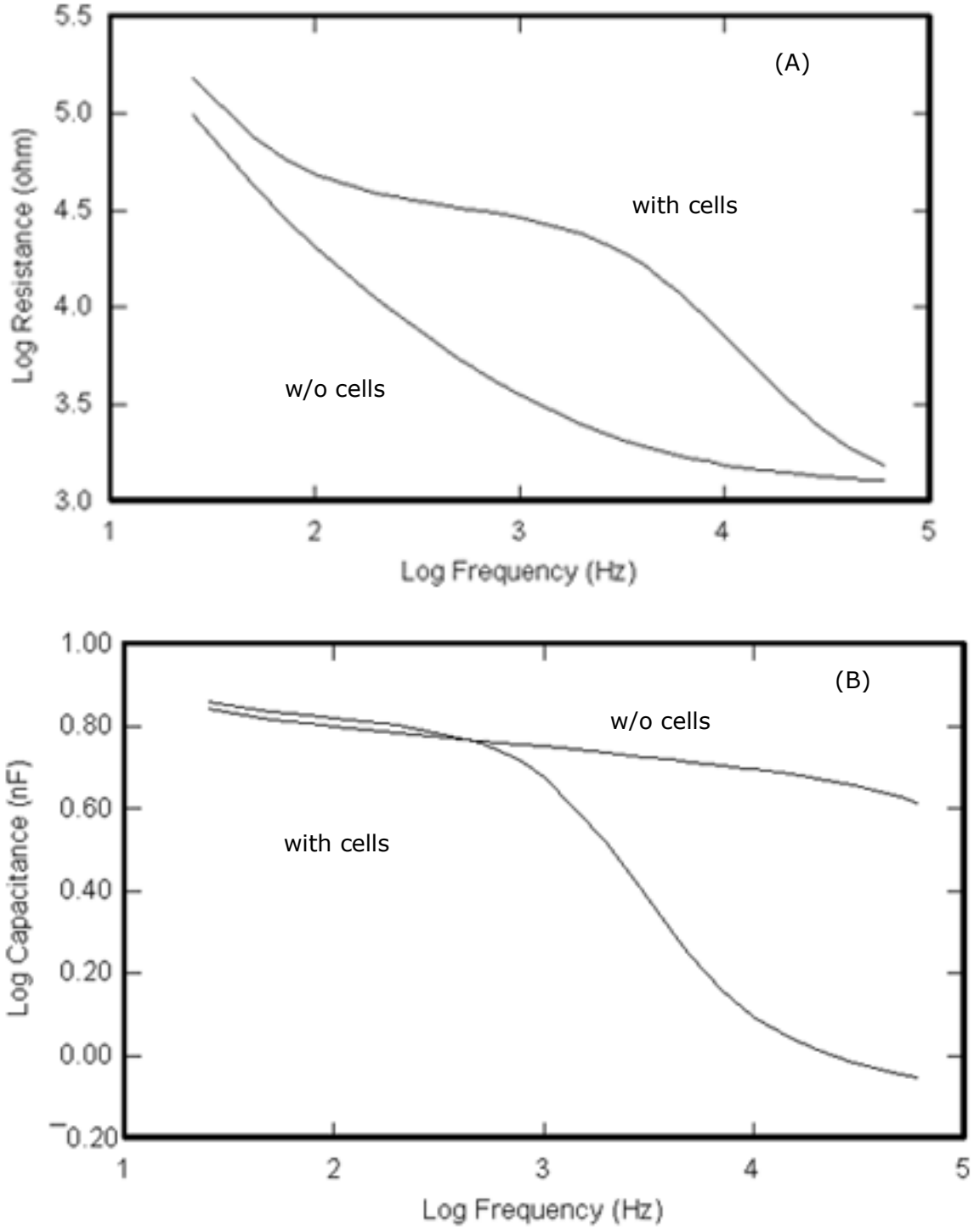

Fig.4.5 (A) Resistance and (B) capacitance data as a function of frequency obtained from Frequency Scan measurement. The data shown is with and without SKOV3 cells in the electrode.

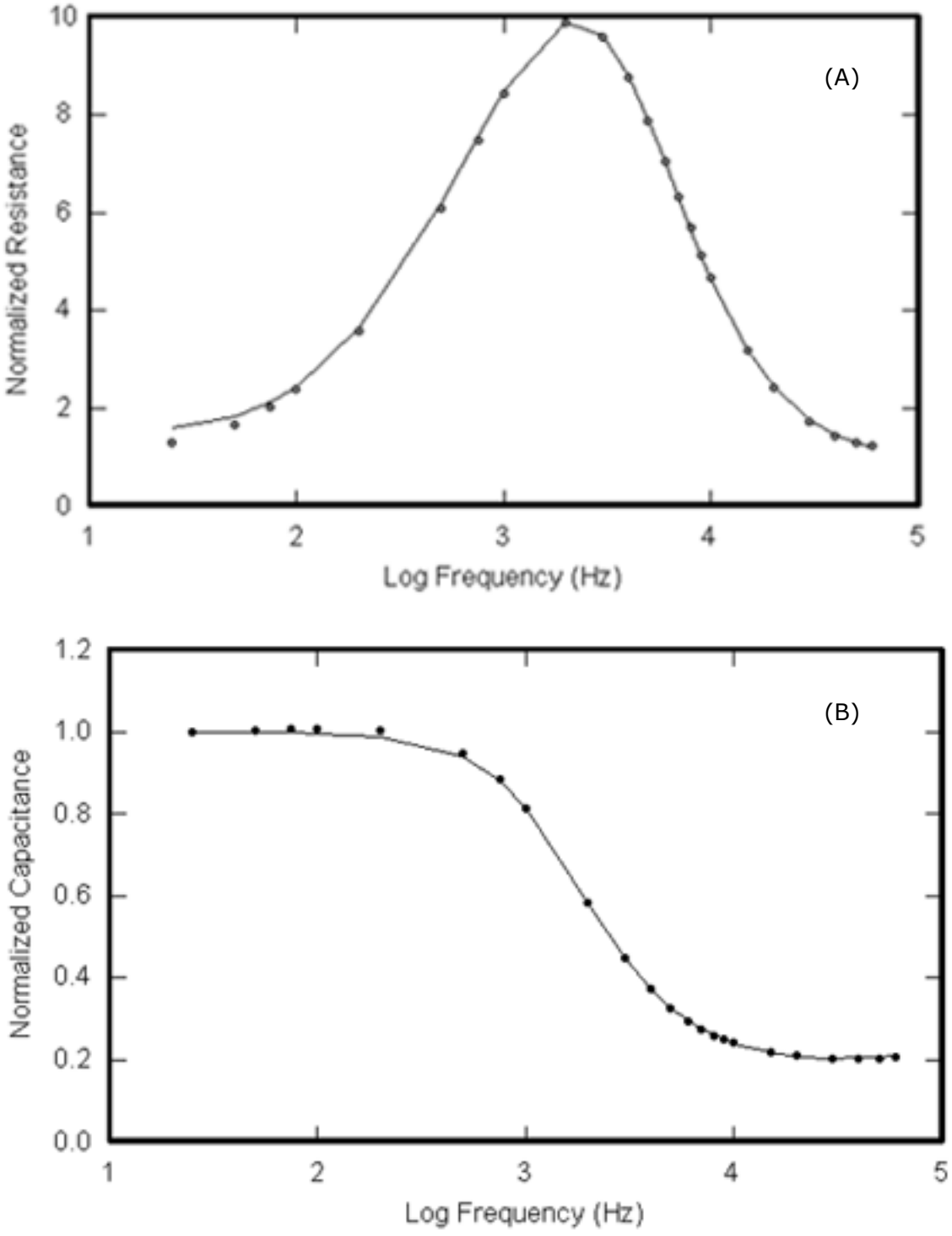

Fig. 4.6 (A) Normalized resistance and (B) Normalized capacitance from model calculation for SKOV3 cells.

Table 4.1.

Impedance analysis of HUVECs, OVCA429, and SKOV3 cells.

	HUVEC (r_c = 20 μm)	*OVCA429* (r_c = 12 μm)	*SKOV3* (r_c = 15 μm)
R_b ($\Omega \cdot cm^2$)	3.9 ± 0.1 (n = 127)	31 ± 4 (n = 47)	7.0 ± 0.6 (n = 53)
α ($\Omega^{1/2} \cdot cm$)	5.2 ± 0.1 (n = 127)	27 ± 2 (n = 47)	5.7 ± 0.2 (n = 53)
h (nm)	94 ± 2 (n = 127)	4.3 ± 1.4 (n = 47)	48.9 ± 3.0 (n = 53)
C_m ($\mu F/cm^2$)	2.4 ± 0.1 (n = 127)	3.8 ± 0.1 (n = 47)	3.6 ± 0.1 (n = 53)

The junctional resistance between cells (R_b), the average cell-substrate separation (h), and the specific membrane capacitance (C_m) were calculated from comparing the experimental data with the calculated values obtained from the ECIS cell-electrode model. The values in this table are means ± standard error.

4.4 Challenge of HUVECs on SKOV3, OVCA429, and HOSE15 cells

After recording the attachment and spreading data for the different cancer cells, we were interested to study how the cancer cells affect the resistance of the normal HUVECs cells. As we understand that if the cells were normal that would increase the resistance when inoculated with HUVECs and if cancer (depends on metastatic and dangerous they are) will drop the resistance. We tried to study the drop in the resistance. We added nearly 10^5 cells/cm^2 of HUVECs in each well of the electrode and allowed the HUVECs to attach to the electrode till it reached the resistance value of nearly 12000 Ω - 13000 Ω. This took approximately two days. We ran the frequency scan to ascertain the resistance value. The frequency scan was ran each time before running challenge experiment. Prior of adding the cancer cells; we first ran the experiment just with the HUVECs in the electrode for 90mins to get the base line. We then added cancer cells to each electrode. One electrode was left as control with just the HUVEC medium without cells. The result is shown in the Fig.4.8. There is a substantial drop in the resistance of wells containing SKOV3, OVCA429 and HOSE15 cells within almost 2 hrs of challenge. This drop is due to the metastatic cells and endothelial monolayer that retracts the endothelial cell junction and interaction of the metastatic cells to the

substratum (21). The sustained reduced resistance after the drop is due the collection of the HUVECs and cancer cell on substratum. The resistance of the well with OVCA429 dropped nearly 50% i.e. from 13000 Ω to 7000 Ω, which shows that this cancer cells break the tight junction between the HUVECs. We see the rise in the resistance value of the OVCA429 cells, which is more than the resistance of the HUVECs. This shows that the OVCA429 penetrate in the HUVEC layer and attach and spread to the electrode. This was really interesting property. The model presented in Fig.4.7 shows how the cancer cells penetrate in the normal HUVEC layer. The resistance ratio from the confluent HUVEC cell layer 5 hrs after exposure to different type of ovarian cancer cells was measured and is given on Table 4.2 The value of R_b and α before and after the challenge of different cancer cell type was also obtained and appears on Table 4.3.

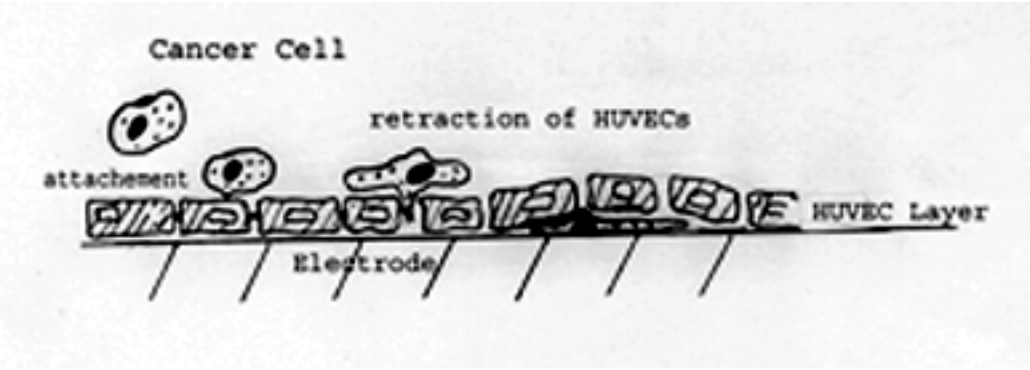

Fig. 4.7 Cancer cell penetration in normal HUVEC cells

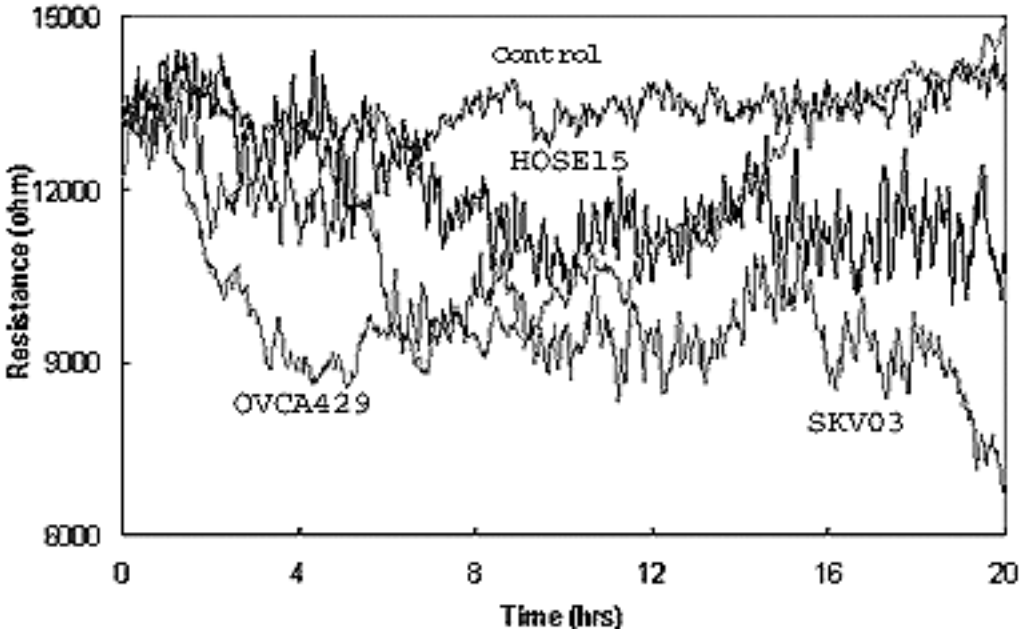

Fig. 4.8 Resistance changes during challenge of HUVEC on SKOV3, OVCA429, and HOSE15 cells. One electrode acts as a control were HUVEC complete medium was placed.

Table 4.2

ECIS data of the resistance ration from confluent HUVEC cell layers 5 hours after exposure to different type of ovarian cells

	HOSE15	*OVCA429*	*SKOV3*
Resistance Ratio	0.90 ± 0.05 (n = 17)	0.69 ± 0.03 (n = 22)	0.82 ± 0.03 (n = 24)

The resistance ratio was calculated from dividing the resistance value at 5 hours after adding ovarian cells by the initial resistance value before adding. The smaller the ratio is, the more invasive the ovarian cells are. The values in this table are means ± standard error. The differences in resistance drop ratio between any two of these three cell types were statistically significant (p = 0.019, 0.006, and 0.002)

Table 4.3.

Change in Model dependent value at different time after the challenge of different cancer cells.

		R_b ($\Omega \cdot cm^2$)	α ($\Omega^{1/2} \cdot cm$)	h (nm)	C_m ($\mu F/cm^2$)
Control	t = 0 hr	3.6	5.2	89	2.4
	t = 20 hr	4.3	5	96	2.4
HOSE15	t = 0 hr	3.8	5.7	74	2.4
	t = 20 hr	1.2	6.2	62	2.1
SKOV3	t = 0 hr	3	5.5	79	2.5
	t = 20 hr	0	5.0	96	2.4
OVCA429	t = 0 hr	3.5	5.7	74	2.4
	t = 20 hr	3.3	7.7	40	2.3

Slight change in the R_b and α with respect to the figure is because a minute change in C_m which was considered constant.

4.5 Effect of Heat-killed Cancer cells on HUVEC layer

As we added large amount of cells during the challenge, we thought that a reaction to the crowded conditions or contact with the cell membranes would have caused the HUVEC cell layer to change. To verify this, we heat-killed the cells by exposure to 55^0 C for 15 mins before adding to the already attached HUVEC cells. The result of this experiments are shown in the Fig.4.9 where established endothelial layers are exposed to cell suspension, one electrode acts as control in which just the HUVEC complete medium is added. The data shows that the heat-killed cells have no effect and are indistinguishable. Moreover the slight drift in the data is due to the decrease in the resistivity of the medium due to evaporation. Thus we showed that heat-killed cancer cells have no effect on the normal HUVEC cells. This is because as we heat-kill the cells, the cells float on the medium and do not attach to the electrode. When viewed through the microscope they were found rounded and floating in the electrode well which confirms that heat-killed cancer cells have no effect on normal HUVEC cells.

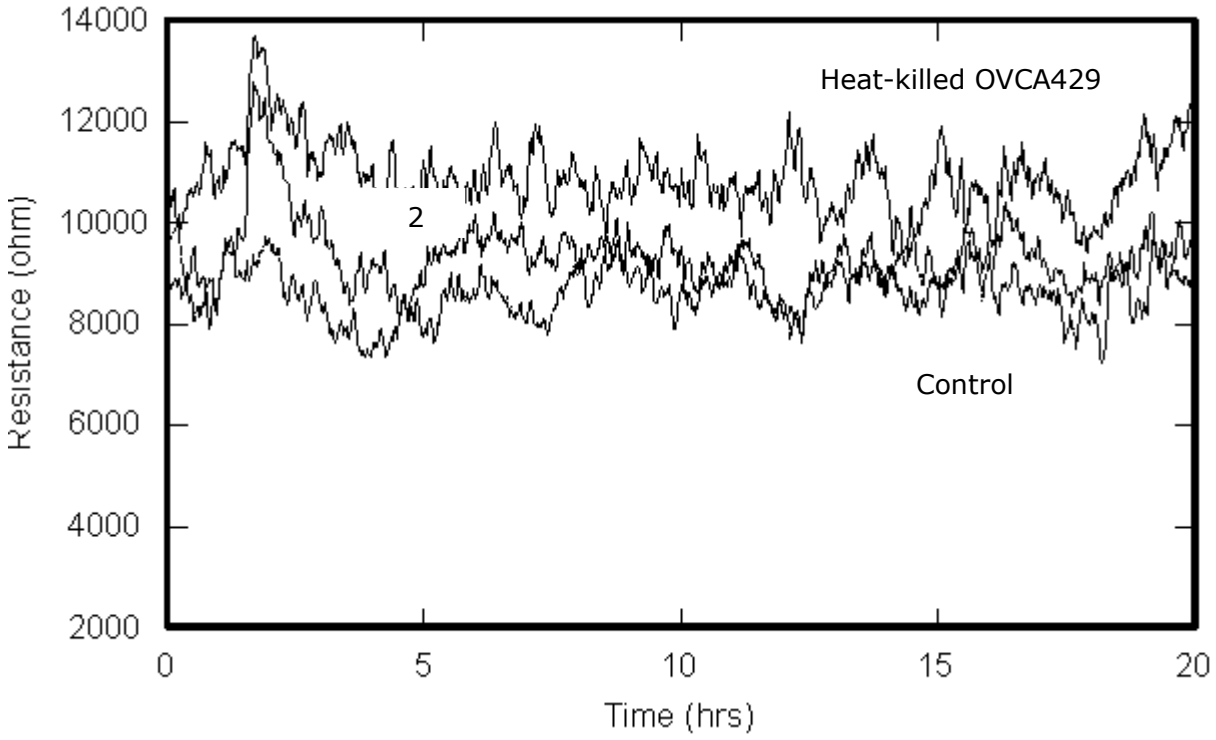

Fig.4.9. Change in HUVEC layer by the challenge of heat-killed OVCA429 and SKOV3 cells. Resistance is at 4 kHz. Number 2 represents SKOV3 conditioned medium.

4.6 Effect of Cancer cell Conditioned Medium on HUVECs

To study the effect of the addition of the soluble solvent released by the metastatic cells on impedance of the HUVECs, we carried out experiment by using conditioned media. The process of obtaining conditioned media is well explained in the above chapter. In this the same amount (as explained above) of HUVEC cells were added to the 0.2ml HUVEC medium. They were allowed to attach and spread for 24 hrs. The frequency scan was then followed to verify the resistance of the HUVEC cells to nearly 12000 Ω. Next, we ran the attachment. Got the baseline nearly 90 min and added 0.25 ml (total volume 0.5 ml) of 3 days conditioned medium obtained from the OVCA429 and SKOV3 cells. One of the electrode served as control were fresh complete medium for growing cancer cells was used. The result is shown in Fig. 4.10. We can conclude from here that the 3 days conditioned medium had no effect on the impedance of the HUVEC cells. Work done with and human pancreatic cells (26) and murine sarcoma cells (25) had shown that conditioned medium by the cancer cell lines caused retraction of endothelial cells. In our experiment we did not see any effect on the HUVEC cells. Slight change may be due to the evaporation of the medium. The overall change was not observed so we can infer that cancer cell conditioned medium had no distinguished effect on the normal HUVEC cells.

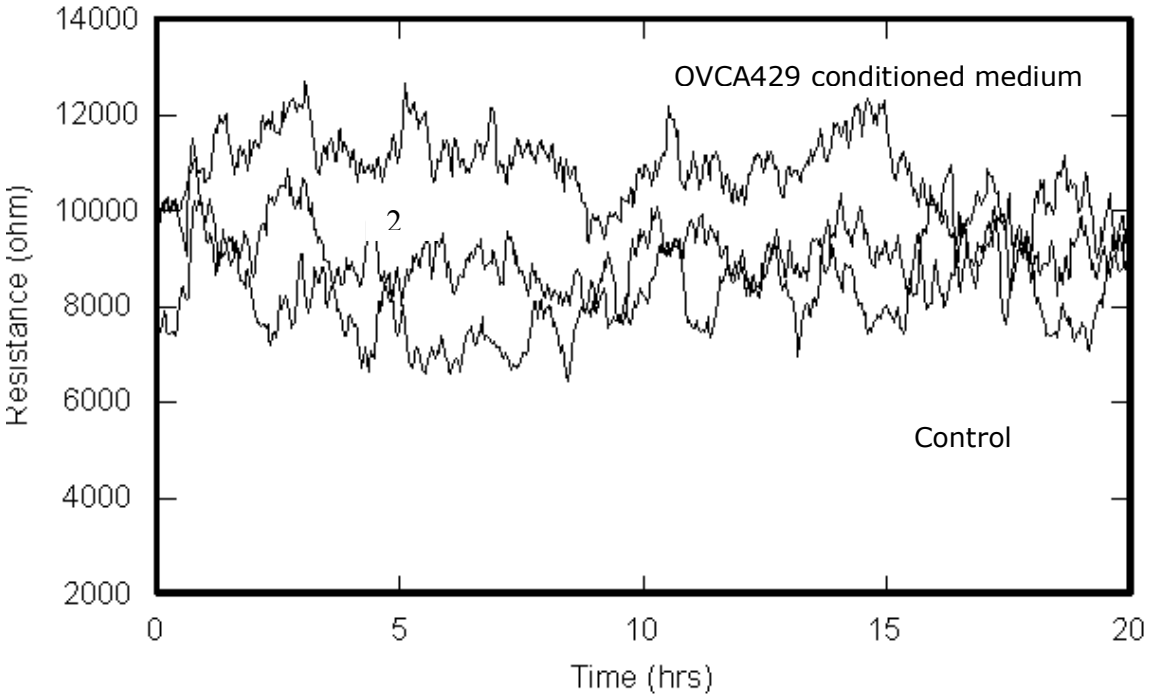

Fig. 4.10. Resistance changes due to conditioned medium. The control received fresh complete medium for growing cancer cell. Here number 2 stands of SKOV3 conditioned medium.

4.7 Interesting effects of OVCA429 cells, 57 hrs after the Challenge

To study the change in resistance value long time after the challenge of OVCA429, the experiment was run for nearly 57 hrs after the challenge of cancer cells. Here we first added 10^5 cells/cm^2 HUVECs each well. Allowed the cells to attach and spread for nearly one day. Then ran the attachment data followed by the frequency scan that served as frequency scan before the attachment data in Fig.4.12. The result of the attachment data is shown in Fig.4.11. Here we see that the resistance drops almost two hours after the inoculation of OVCA429 cells. This shows that the cancer cells break the tight junction of the HUVEC cells and as described in the Fig.4.7, the cancer cells tries to attach at the electrode by penetrating in the HUVEC layer. We observed sudden rise in resistance value after 20 hrs of challenge. This rise cannot be because the HUVEC cells resealed because the resistance of the HUVECs is approximately 12000 Ω while the rise in the resistance is to 17000 Ω. So we can say that the rise in the resistance is due to the tight junction of the OVCA429 cells. To confirm this we had the frequency scan data before the challenge of OVCA429 cells, 20hrs after the challenge and 56 hrs after the challenge of OVCA429 cells. The resistance ratio is shown in the Fig.4.12 at different time. From the figure, we observe the decrease in the

resistance ratio after 20 hrs of challenge, which is due to the retraction of the HUVECs from the electrode. The sudden rise in the resistance ratio after 57 hrs of challenge is due to the rise in the R_b value. By the model explained above the best fit of the data in Fig.4.12.is obtained for R_b=1.6 Ωcm^2, α=5.9 $\Omega^{1/2}$cm, and C_m=2 $\mu F/cm^2$ before the challenge of OVCA429. Twenty hours after the challenge we see the best fit is obtained with the value of R_b=1.5 Ωcm^2, α=5.2 $\Omega^{1/2}$cm, and C_m=2.1 $\mu F/cm^2$. To see the final change we even obtained the best-fit to the data obtained 57 hrs after the OVCA429 cell challenge. The best fit for this fit was obtained for R_b=4.9 Ωcm^2, α=7.7 $\Omega^{1/2}$cm, and C_m=2.4 $\mu F/cm^2$. Thus we see large change in R_b, which is due to the retraction of HUVEC cells. Similarly we had carried different experiments with SKOV3 and HOSE15 cells, the data not shown. The change in barrier function (R_b) and alpha (α) is shown in Fig. 4.13 and Fig.4.14. These values were obtained from the computer software by plugging the values of resistance and membrane capacitance. In both the figure, the (A) part is for first 20 hrs and (B) part is after 20 hrs, 40 mins (paused for frequency scan). The values obtained aggress with the data shown in figure 4.11. All the above results obtained by ECIS method were consistent and in good agreement with the theory. We can use this method to even study different cell types.

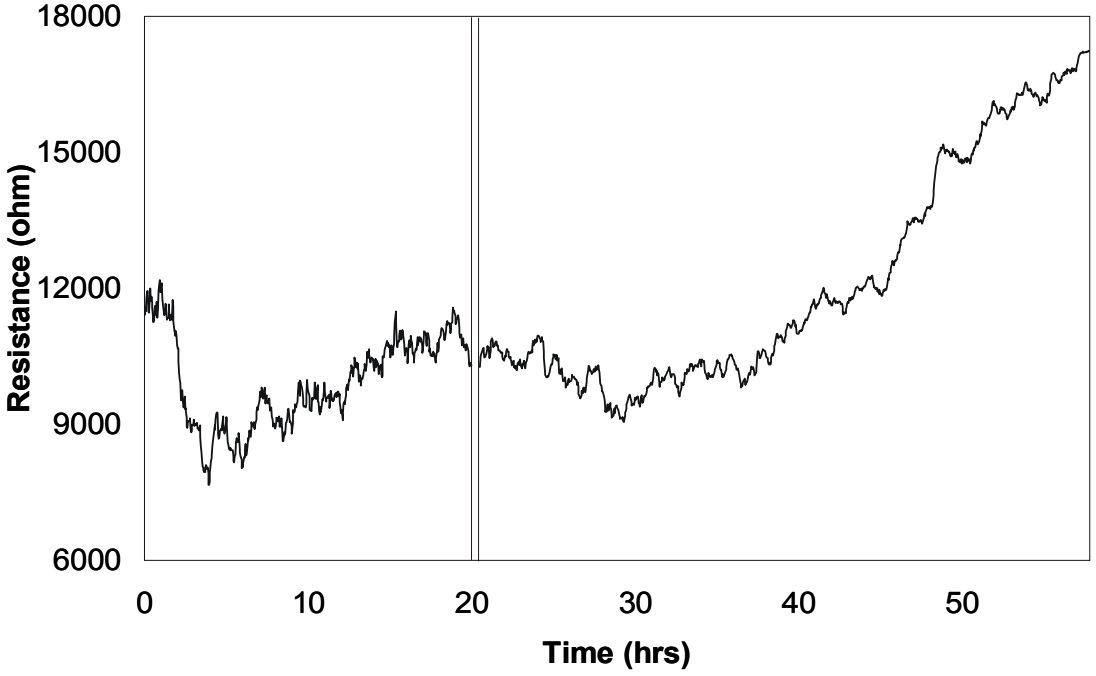

Fig 4.11. Change in resistance after the challenge of OVCA429 cells. At vertical line the experiment was paused to get the frequency scan data.

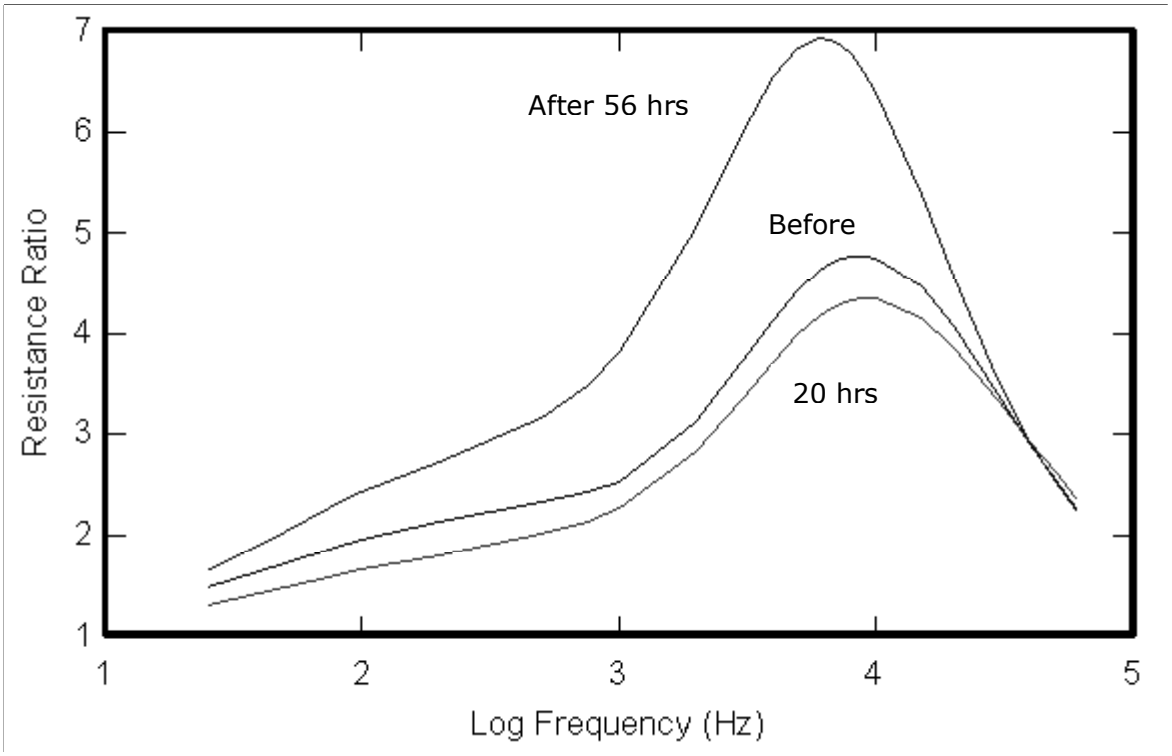

Fig.4.12 Change in the resistance ratio at different time after the challenge of OVCA429 cancer cells. Here before represents the ratio before the challenge of OVCA429 cells when only the HUVEC cells were present, 20hrs means, the ratio of with and without cells 20 hrs after the challenge of OVCA429 cells. After shows the ratio 56 hrs after the challenge of OVCA429 cells.

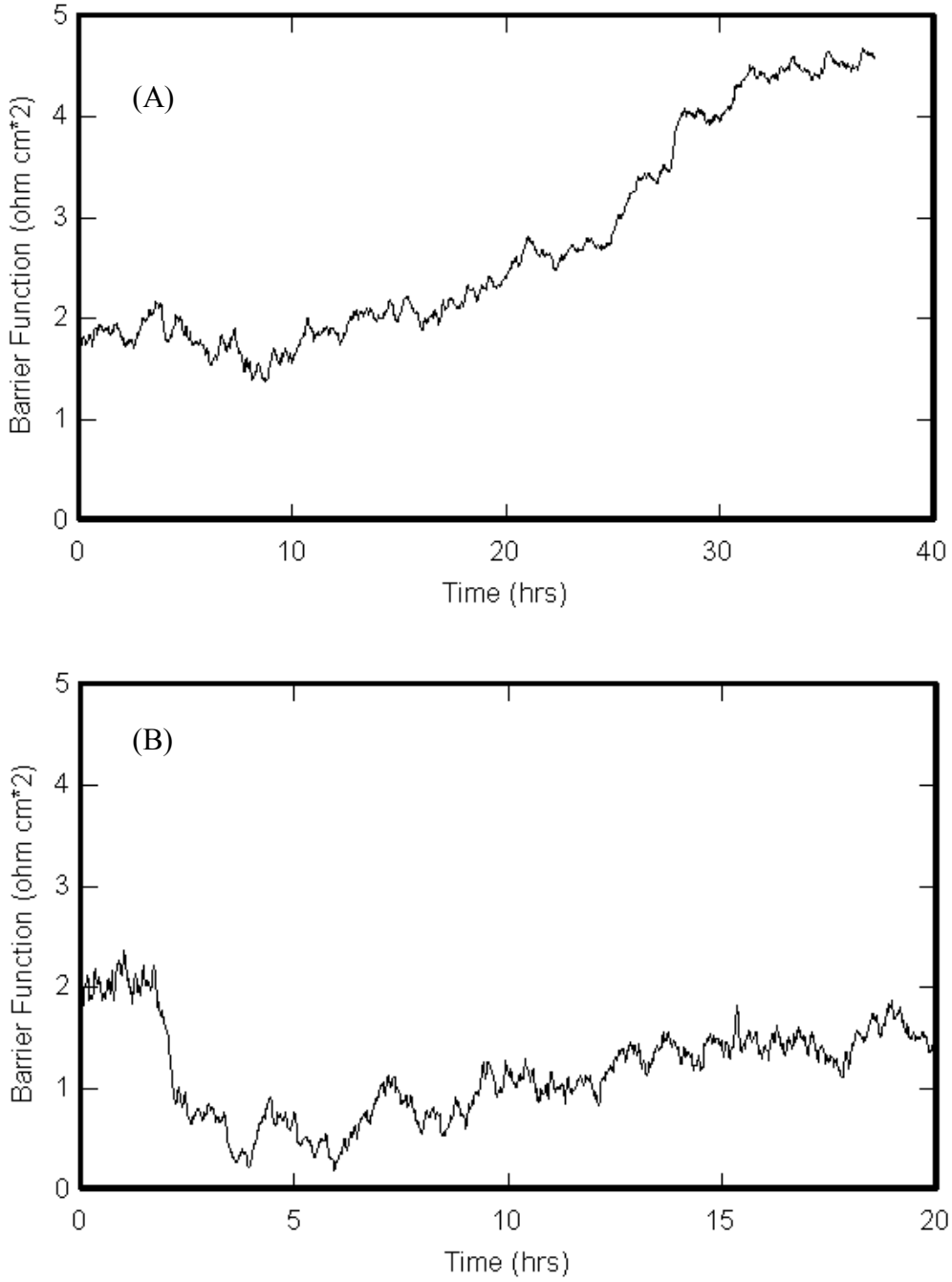

Fig.4.13 Change in the barrier function (R_b) as function of time during the challenge of OVCA429 cells. The Fig. (A) represents the first 20 hrs and (B) next 20 hrs after the OVCA429 challenge.

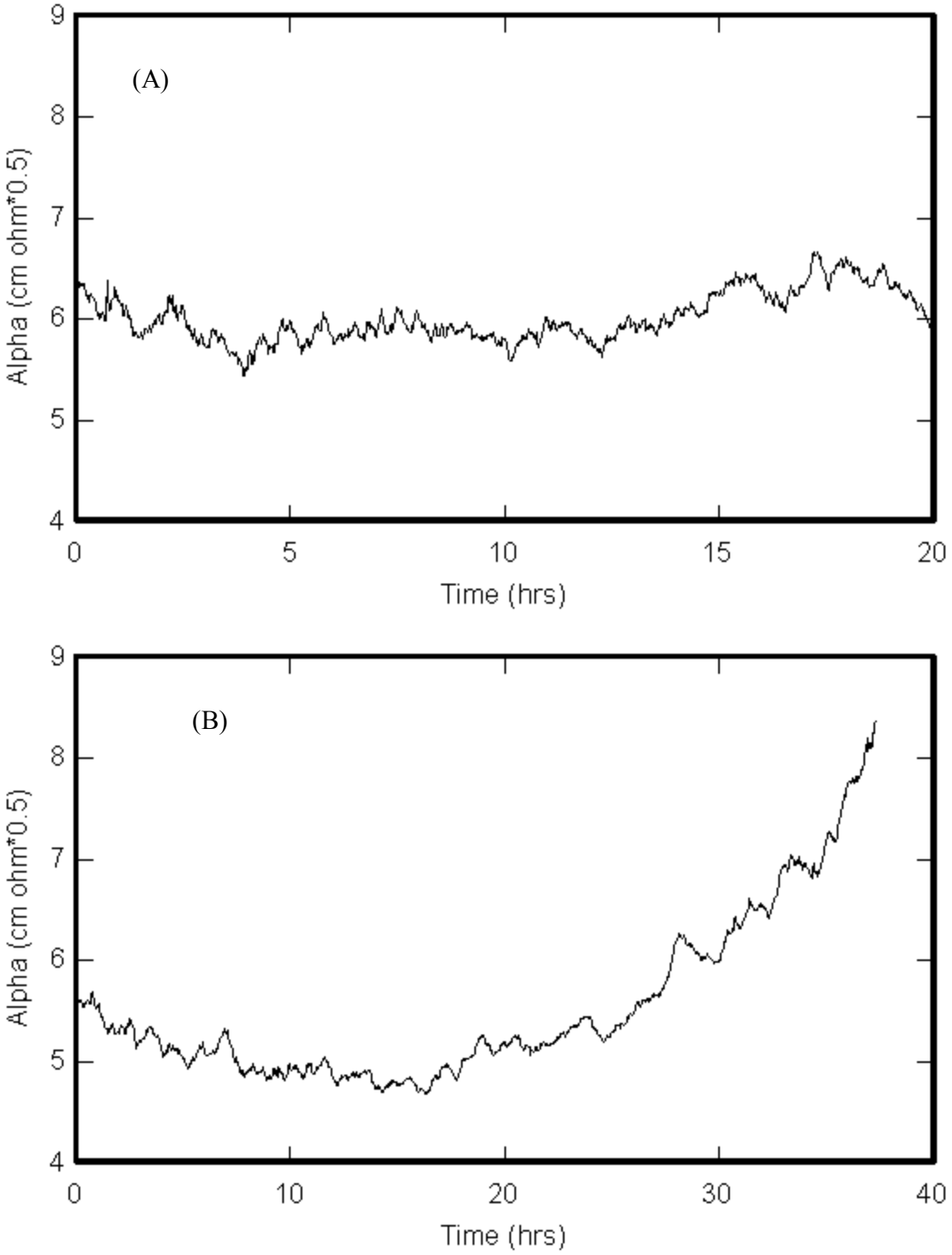

Fig.4.14 Challenge in model parameters by OVCA429 cell challenge. The change in alpha is based on model of cell-induced impedance changes. The (A) part is for first 20 hrs after challenge of OVCA429 cells and (B) is the change in α after 20hrs.

Chapter 5

SUMMARY AND FUTURE ASPECT

5.1 Summary

In the summary, I would like to give the brief outline of the work done in our lab and in future aspect would outline the work to be done in our lab.

In our lab we used the polystyrene dishes with culture medium to grow the SKOV3, OVCA429 and HOSE cells but the HUVECs did not attach very well to the culture dish so the flask with tissue culture medium was used to culture them. Cells were then added to the dish/flask as suspension and kept in the incubator at constant temperature of 37^0C and 5% CO_2 to adjust pH of the mediums buffering system. The cells are usually spherical on the top of the dish and gets flattened on reaching the substrate as the begin attaching. This process takes 2-3 hours for most commonly cultures cells. The individual cells then grows and divide. The daughter cell again spreads out, divide and continue the cycle till the dish is full confluent. Usually depending in the number of suspended cells, the culture dish get confluent. Once the culture dish is confluent, the cells are they

subcultured after being trypsinized. HUVECs, SKOV3, OVCA429 and HOSE15 cells can be cultured and studied in the vitro. In our lab we used ECIS to study the noninvasive activity of the cells. We usually used HUVECs till passage 6 and ovarian cancer cells till passage 12. The cells were suspended on the evaporated gold electrode. The behavior of the cells is reflected in the measured impedance by using a lock-in amplifier. Voltage and phase data are stored and processed with a personal computer that controls the output of the amplifier and switches the measurement to different electrodes at various time during the measurement. This method thus provides the quantitative information of cell substrate interaction in real time. Moreover the current and voltage applied to the cell layer is sufficiently low so it does not affect the cell and can hopefully lead to many applications in future. A theoretical cell electrode model is developed in chapter 3, where the cells are regarded as spherical. The frequency scan and the attachment data obtained were excellent. Through the ECIS measurements we were able to detect the R_b and α of the SKOV3 and OVCA429. We found that the R_b and α for OVCA429 was higher than SKOV3 which may shows that the invasive activity of OVCA429 was too high and can penetrate inside the HUVEC cell layer. Thus we can conclude that ECIS can be very useful to study the cell morphology of different cell type.

5.2 Future Aspect

In our laboratory we study the motility and viability of different cells. The computer program analyzes our ECIS results. The future aspect of our research is to study how fluid flow influence the invasive activity of ovarian cancer cells and to test anticancer drug to study its effect on the challenge of HUVECs. We are even looking forward to try different cell types like muscle cells and kidney cells.

References

1. Hahnfeldt, P., D.panigrahy, J.Folkman, and L.Hlatky.1991.

   Tumor development under angiogenesis signaling: A dynamic theory of tumor growth, post-vascular dormancy and treatment response.

   Cancer Res.59:24770-4775.

2. Lafrenie, R.M., T.J. Podoe, M.R. Buchanan, and F.W.Orr.1992.

   Up-regulated biosynthesis and expression of endothelial-cell vitronection receptor enhances cancer cell adhesion.

   Cancer Res.52:2202-2208..

3. Honn, K.V.,D.G. Tang, I. Grossi, Z.M.Duniec, J. Timar, C.Renaud, M.Leithauser,I.Blair,etal.1994.

   Tumor cell derived 12(S)-hydroxyeicosateraenoic acid induces microvascular endothelial-cell retraction.

   Cancer Res.54: 564-574.

4. Charles R. Keese, Kaumudi Bhawe, Joachim Wegener, and Ivar Giaever. 2002

   Real-Time impedance assay to follow the invasive activities of metastatic cells in culture.

   BioTechniques 33:842-850

5. Kelli Solly et al. 2004

Application of real-time cell electronic sensing (RT-CES) technology to cell based assay.

Assay and Drug development Technology, Vol-2 Number 4,

6. Misfledt, D.S.Hamamoto,S.T.&Pitelka, 1978

D.R.(1976)Proc.Natl.Acad.Sci.US73,1212-1216

Cereijido,M.,Robbins,E.S., Dolan,W.J.,Rotunno,C.A.& Sabatini,D.D J.Cell Biol.77,853-880).

7. I.Giaever and Keese (1984)

Monitoring fibroblast behavior in tissue culture with applied electric field. Proc.Natl.Acad.Sci.Vol.81, pp.3761-3764.

8. Thomas, C.A., Jr., Springer, P.A., Loeb,G.E.,Berwald-Netter,Y & Okum,L.m. (1972)

Exp. Cell.Res.14,61-66)

9. Wegener, Keese and Giaever (2000)

Electric cell substrate impedance sensing as a noninvasive means to monitor the kinetics of cell spreading to artificial surface.

Experimental Cell Research 259, 158-166

10. Ghosh, P.M, C.R.Keese.1994.

Morphological response of mammalian cells to pulsed ac field. Bioelectrochem. Bioenergetics 33:121-131).

11. Ivar Giaever and Charles Keese (1991)

Micromotion of mammalian cells measured electrically

Proc.Natl.Acad.Sci.Vol.88, pp.7896-7900.

12. Partin, A. W., Isaac, J. T., Treiger, B. & Coffey, D. S. (1988)

Cancer Res. 48, 6050-6053.

13. Partin, A. W., Schoeniger, J. S., Mohler, J. L. & Coffey, D. S.

(1989)

Proc. Natl. Acad. Sci. USA 86, 1254-1258.

14 .Brady-Kalnay, S. M., Soil, D. R. & Brackenbury, R. (1991)

Int. J. Cancer 47, 560-568.

15. Lo, C.M., C.R.Keese and I.Giaever. 1993.

Monitoring motion of confluent cells in tissue culture.

Exp. Cell Res.204:102-109

16. Ivar Giaever and Charles Keese, 1991

Micromotion of mammalian cells measured electrically)

Proc. Natl. Acad. Sci USA Vol. 88, pp. 7896-7900,.

17. Holm, Englewood Cliffs, NJ), pp. 152-181.

18. Hildebrand, F. B. (1948)

Advanced Calculus for Engineers

(Prentice-Hall, Englewood Cliffs, NJ), pp. 152-181.

19. Warburg, E. (1901)

Ann. Phys. 6, 125-135.

20. Onaral, B., Sun, H. H. & Schwan, H.P. (1984) IEEE Trans. Biomed

Eng. 31, 827-832.

21. Charles Keese Kaumudi Bhawe, Joachim Wegener and Ivar Giaever (2002)

Real Time Impedance Assay to Follow the Invasive Activities of Metastatic Cells in Culture.

BioTechniques 33:842-850

22. Chun-Min Lo and Jack Ferrier (1998)

Impedance Analysis of Fibroblastic Cell Layers Measured by Electric Cell-Substrate Impedance Sensing.

The American Physical Society.Phy Rew. E

23. Joachim Wegener, Charles R. Keese, and Ivar Giaever (2000)

Electric Cell-Substrate Impedance Sensing (ECIS) as Noninvasive means to Monitor the kinetics of Cell Spreading to Artificial Surfaces

Experimental Cell Research 259, 158-166

24. Giaever, I. and Keese C.R., (1986).

Use of electric fields to monitor the dynamical aspect of cell behavior in tissue culture.

IEEE Trans.Biomed. Eng. 33: 242-247

25. Yasuda, T., H. Matsui, M Kanamori, Yudoh, K. Ohmori, M. Aoki, and H. Tsuji. 1999.

Effects of tumor cells-derived interleukin 1 alpha on invasiveness of

metastatic clones of murine RCT sarcoma through endothelial cells. Tumor Biol. 20.105-116.

26. Mitra, P., C.R.Keese, and I.Giaever.(1991) Electric measurements can used to monitor the attachment and spreading of cells in tissue culture. BioTechniques 11:504-511.